

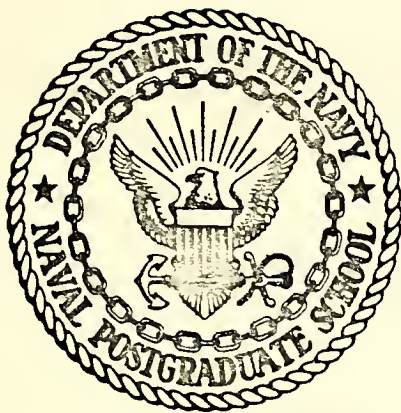
**A THEORETICAL STUDY OF METEOROLOGICAL
EFFECTS OF THE DISPERSION OF ATMOSPHERIC
CONTAMINANTS IN THE COASTAL ENVIRONMENT**

Michael Alan McCallister

Library
Naval Postgraduate School
Monterey, California 93940

NAVAL POSTGRADUATE SCHOOL

Monterey, California



THESIS

A THEORETICAL STUDY OF METEOROLOGICAL
EFFECTS ON THE DISPERSION OF ATMOSPHERIC
CONTAMINANTS IN THE COASTAL ENVIRONMENT

by

Michael Alan McCallister

Thesis Advisor:

C. L. Taylor

MAR 1974

Approved for public release; distribution unlimited.

7159114

A Theoretical Study of Meteorological
Effects on the Dispersion of Atmospheric
Contaminants in the Coastal Environment

by

Michael Alan McCallister
Lieutenant, United States Navy
B.S., Oregon State University, 1965

Submitted in partial fulfillment of the
requirements for the degree of

MASTER OF SCIENCE IN METEOROLOGY

from the

NAVAL POSTGRADUATE SCHOOL
March 1974

Thesis
MIGASS
c.2

ABSTRACT

Present numerical models describing pollutant diffusion employ two main approaches to the problem. Gaussian bivariate distributions based on the statistical properties of atmospheric flow have the advantages of simplicity and computational economy. Numerical simulations of diffusion, based on the continuity equation and conservation relations, allow a more precise description of atmospheric turbulent flow.

The thesis examines numerical models of each method. The governing equations are discussed, with basic assumptions which permit reasonable simplifications to be made. Results of both models are examined qualitatively to describe patterns of marine-layer pollutant dispersal. Calculations from both models reveal wind velocity to be the most critical atmospheric characteristic controlling dispersion. Rates of spreading are also closely related to other measurable meteorological properties such as thermal stability and mixing depth.

TABLE OF CONTENTS

I.	INTRODUCTION -----	8
II.	PURPOSE -----	12
III.	DESCRIPTION OF THE COASTAL ZONE -----	13
	A. MONTEREY BAY CIRCULATION -----	13
IV.	MODEL DEVELOPMENT -----	17
	A. BASIC ASSUMPTIONS -----	17
	B. GAUSSIAN MODEL -----	17
	C. AN ALTERNATE MODEL -----	22
	1. Boundary Conditions -----	23
	2. Formulation of Numerical Model -----	23
	3. Implicit Methods -----	24
V.	MODEL APPLICATION -----	26
	A. SOURCE DATA -----	26
	B. GAUSSIAN MODEL -----	26
	1. Grid -----	26
	2. Meteorological Data -----	26
	a. Wind Field -----	26
	b. Atmospheric Stability and Dispersion Coefficients -----	28
	C. ALTERNATING DIRECTION IMPLICIT MODEL -----	30
	1. Grid and Timestep -----	30
	2. Meteorological Conditions -----	31
	a. Wind Field -----	31
	b. Atmospheric Stability -----	33
	c. Diffusion Coefficients -----	34

VI.	RESULTS -----	37
A.	GAUSSIAN MODEL -----	37
B.	ADI MODEL -----	40
C.	DISCUSSION OF RESULTS -----	49
VII.	CONCLUSIONS AND RECOMMENDATIONS FOR FUTURE STUDY -	52
APPENDIX A	ATMOSPHERIC SULFUR DIOXIDE: GENERAL CONSID-	
	ERATIONS -----	56
	BIBLIOGRAPHY -----	59
	INITIAL DISTRIBUTION LIST -----	62
	FORM DD 1473 -----	63

LIST OF TABLES

TABLE

I.	PLUME RISE -----	21
II.	THEORETICAL POWER PLANT SPECIFICATIONS -----	27
III.	STABILITY CLASSIFICATION -----	29

LIST OF FIGURES

FIGURE

1.	GAUSSIAN PLUME MODEL -----	10
2.	SOUTH MONTEREY BAY TOPOGRAPHY -----	14
3.	ADI VELOCITY PROFILES -----	32
4.	ADI DIFFUSION COEFFICIENTS -----	36
5.	DOWNWIND SO ₂ CONCENTRATION AS A FUNCTION OF STABILITY -----	38
6.	DOWNWIND SO ₂ CONCENTRATION AS A FUNCTION OF MARINE LAYER DEPTH -----	39
7.	DOWNWIND SO ₂ CONCENTRATION AS A FUNCTION OF WIND VELOCITY -----	41
8.	PEAK GROUND-LEVEL CONCENTRATION: $\mu\text{gm}/\text{m}^3$ -----	42
9.	DISTANCE TO PEAK GROUND-LEVEL CONCENTRATION FROM SOURCE: km -----	43

ADI MODEL FIGURES

10.	FICKIAN DIFFUSION -----	45
11.	S=3, U ₁₀ = 10 mps -----	46
12.	S=4, U ₁₀ = 10 mps -----	47
13.	S=3, U ₁₀ = 5 mps -----	48

ACKNOWLEDGEMENT

The author wishes to express his gratitude to the following members of the Naval Postgraduate School Meteorology Department: Professor G. J. Haltiner, Chairman; Professors C. P. Chang, K. L. Davidson, R. L. Elsberry, R. L. Haney, F. L. Martin, R. J. Renard, C. L. Taylor and R. T. Williams. The guidance and instruction provided by these men during the writer's tenure as a student at NPS has been sincere and expert. An additional word of thanks is due to Distinguished Professor F. D. Faulkner and Professor D. A. Archer of the Mathematics Department for their advice regarding the ADI model described in this thesis.

The author also desires to acknowledge the patience and assistance of his wife, Nancy, through four and one-half years of graduate study.

I. INTRODUCTION

The use of computer simulation techniques has in recent years greatly enhanced the exploitation of existing theoretical knowledge in the analysis of physical phenomena. The development and application of numerical predictive models is now routine in many scientific and technical fields, including airshed management. Such models can be used to study the complicated relationship between air quality and emission sources as a function of meteorological parameters, topography and time.

The goal of research in this field is the accurate prediction of pollution levels and, ultimately, air quality management. However, before prevention of harmful pollution episodes by regulation of sources is feasible, an adequate real-time forecast system must be developed. In addition to "red-flagging" pollutant concentrations in excess of levels toxic to living organisms, this scheme should have the capacity to designate:

1. the optimum loci and times of day at which atmospheric injection of pollutants will be least damaging to air quality;
2. the relative effectiveness of various control measures on a particular source.

The success of such a control model on either a local or regional basis depends primarily upon the reliability of diffusion estimates calculated by the method. Given the

current state of diffusion modeling, the achievement of these goals is not likely for some time to come. Present models are formulated from the concentration equation governing the various pollutant species. In theory this equation can be solved using known source emission rates, meteorological parameters, horizontal and vertical boundary conditions, turbulent transport rates and chemical reactivity. Practically, however, present data acquisition falls far short of the necessary detail for a valid solution to the equation. As a consequence, various restricted but more tractable models have been developed, based upon statistical theory and simplifying assumptions. The two most common approaches today are Gaussian diffusion and numerical simulation.

The Gaussian plume (steady-state) and puff (dynamic) models describe the concentration distribution of inert constituents and are derived from the stochastic continuity equation under homogeneous, isotropic conditions. Downstream from a point source the average concentration on a crosswind plane is assumed to fit a normal bivariate statistical distribution (Figure 1). Observations indicate that this approximation is reasonable only for very short-term forecasts. However, the shortage of detailed meteorological data and the simplicity and computational economy of Gaussian methods have motivated their continued popularity. The models of Pasquill [1961], Turner [1964], Hilst [1967], and Johnson [1970] are representative examples.

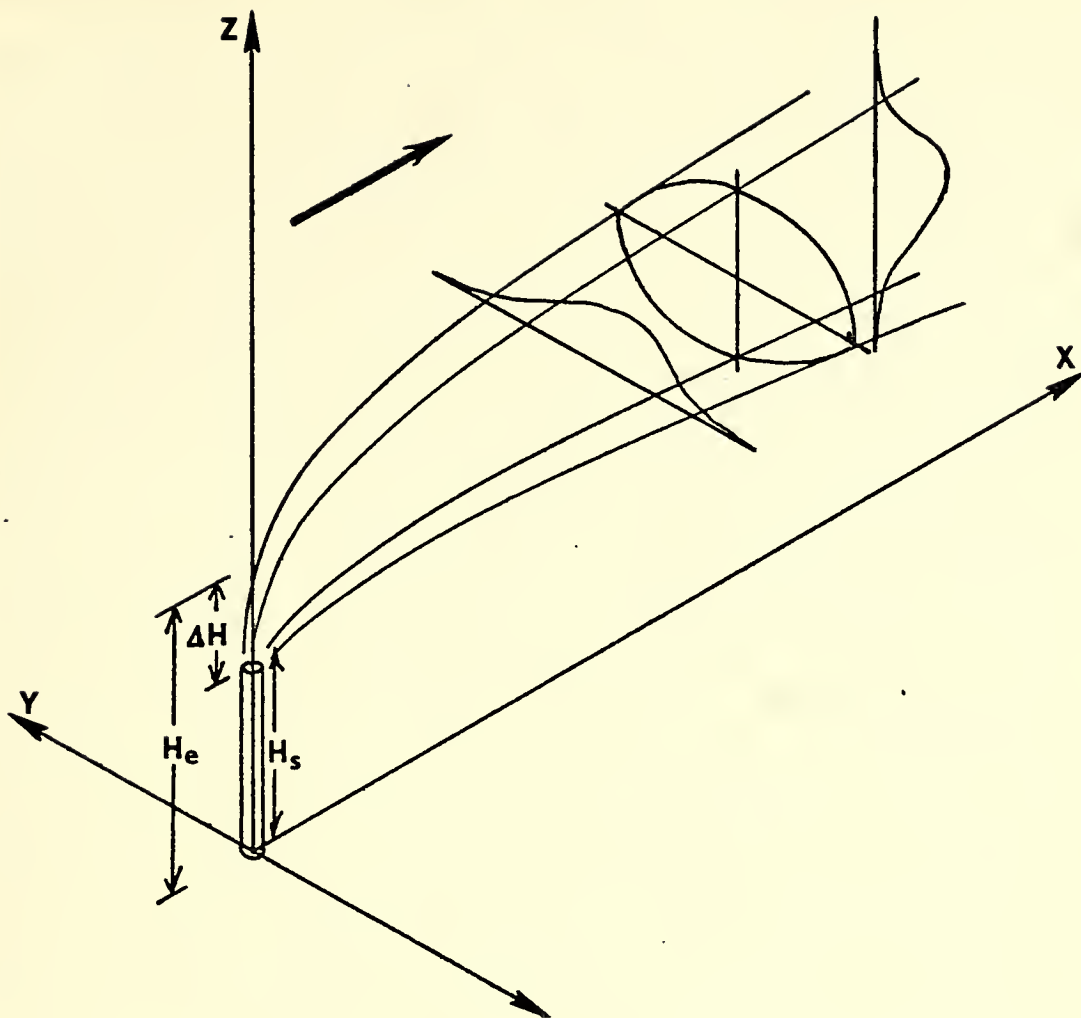


FIGURE 1 GAUSSIAN PLUME MODEL

Most statistical formulae are limited in their application by failure to consider chemical alterations of pollutant species. Some atmospheric constituents react chemically or photochemically with others, yielding entirely new compounds. Deposition and absorption at the earth's surface and washout by aerosols reduce concentrations. Further, the normal statistical distribution accurately applies only to continuous sources emitting into a steady laminar flow. Conditions of zero wind or weak winds can result in singularities. The complex nature of thermally- or topographically-induced turbulence and wind shear can only be crudely approximated for incorporation in Gaussian models.

Atmospheric pollutant dispersion is more adequately described by numerical simulation of concentration diffusion. Simplified forms of the continuity equation have been applied by Randerson [1970], Lamb [1971], and Shir et al [1973] to form the bases for multiple source urban diffusion models. As yet, however, the closure problem encountered in limiting the degrees of freedom of the turbulent system still looms as an insurmountable problem.

II. PURPOSE

The primary objective of this thesis is to study the importance of meteorological conditions in the prediction of pollutant dispersal. Variations of wind velocity, atmospheric stability and mixing-layer thickness are considered. Meteorological effects on dispersion are examined for both a simple Gaussian formula and for a model based on a more complete form of the concentration diffusion equation.

Most present models distinguish between area and line sources of pollution, such as clustered home heating units and freeways, from the emissions of major atmospheric outfalls such as power plant stacks. Area and line contributions can be regarded as the integral of numerous small point sources over a particular region and as such are separable from large-point contributions.

The single most significant cause of air pollution in many cities is the generation of electrical power by combustion of fossil fuels. This thesis therefore considers contaminants from a large point source only, neglecting area and line contributions. Furthermore, since nearly fifty percent of all power produced in the United States is generated on the coastal plain, the study is applied to that zone (specifically the Monterey Bay region).

III. DESCRIPTION OF THE COASTAL ZONE

In the transition zone between marine and continental airsheds, both natural inhomogeneities in temperature, density and moisture, and human activities contribute to the concentration of atmospheric contaminants. An airmass flowing across the coastline encounters a step change in surface roughness and frequently in temperature as well. The dynamical and thermal response of the atmosphere to these changes in the properties of the underlying terrain is the downstream propagation of turbulence in the boundary layer.

The rate of diffusion of airborne pollutants, particularly in the vertical, depends primarily upon the turbulent character of the atmosphere. Turbulence is controlled by the wind velocity, static stability, nature of terrain, degree of surface heating, lateral boundaries, existence of inversion layers and other factors of local significance. The result is a reduction in mixing time in the coastal zone marine layer, enhancing the distribution of contaminants.

A. MONTEREY BAY CIRCULATION

The geography and topographic relief of the Monterey Bay region are shown in Figure 2. Although this study is theoretical in that no attempt is made to correlate findings with actual source inventory data or measured pollution levels, the thesis models are designed to represent as closely as possible the meteorological features of the locale.

Darling [1971] has shown that for the South Monterey Bay the low-level atmospheric circulation is almost totally topography-dependent, with little contribution by meso- and synoptic-scale circulatory patterns. Read [1972] found the surface wind field at Moss Landing to be essentially representative of the undisturbed offshore flow. Circulation in the north and south parts of the bay is dominated by divergent topographically-induced eddies.

The characteristic daytime thermal structure of the surface boundary layer exhibits a dry inversion near 600 meters throughout much of the year. Cool marine air intrudes along the coastline in the early morning, wedging the faster-warming continental airmass upward. The inversion forms at the interface between these two bodies of air and is usually intensified by subsidence of warm dry air from the eastern cell of the Pacific Subtropical Ridge. The turbulent, well-mixed marine layer increases in depth early in the day, reaching a maximum thickness first at the coastline and later inland; depth of the layer decreases in the afternoon. Schroeder et al [1967] related the depth of the marine air-mass directly to the wind velocity.

The predominant local wind and thermal patterns thus affect the dispersal and transport of pollutants in two ways. Contaminants are first distributed fairly uniformly throughout the nearsurface air column, or marine layer. Further vertical transfer is then inhibited by the inversion, while lateral mixing continues until homogeneity is attained.

In winter, the above pattern is completely disrupted by the passage of migratory cyclones. However, during these times the marine layer is extremely deep and pollution is not nearly as much of a problem.

IV. MODEL DEVELOPMENT

A. BASIC ASSUMPTIONS

Since pollutants occur at concentrations of no more than a few parts per million in the Monterey Bay atmosphere, their presence can be assumed to have no effect on the meteorological conditions. Additionally it must be recognized that the incorporation of spatial photochemistry (chemical reactivity of pollutant species) in a dispersion model is a complete subject for research in itself. Thus the concentration of a relatively nonreactive constituent, sulfur dioxide, is used in this study to model the diffusion of all contaminants. If the basic model can accurately predict SO_2 concentrations, chemical constraints may later be considered.

Atmospheric flow is assumed to be incompressible and to obey the laws of conservation of mass, momentum and energy. Wind is given as a function of x , y and t , but is considered to be independent of height and invariant in the vertical coordinate only above a friction layer, the depth of which is related to surface roughness.

B. GAUSSIAN MODEL

The concentration of SO_2 in the atmosphere must satisfy the continuity equation, written in flux form as:

$$\frac{\partial C}{\partial t} + \nabla \cdot (\vec{V}C) = R + Q + D\nabla^2 C \quad (1.1)$$

where

C = concentration of SO₂ at a point;

R = time rate of change of concentration due to photo-chemical reaction;

Q = source intensity;

D = molecular diffusivity of SO₂.

The evolution of the velocity components u, v and w can be approximated by the Navier-Stokes equations for a nonrotating, incompressible Newtonian fluid. Conversion of these equations from Cartesian tensor form as expressed by Monin and Yaglom [1965, Eq. 1.6] to vector flux form yields:

$$\frac{\partial \vec{V}}{\partial t} + (\vec{V} \cdot \nabla) \vec{V} = -g\vec{k} - \frac{1}{\rho} \nabla p + \nu \nabla^2 \vec{V} . \quad (1.2)$$

The system of equations is completed by the continuity equation:

$$\nabla \cdot \vec{V} = 0, \quad (1.3)$$

and the equation of state:

$$p = \rho RT . \quad (1.4)$$

The wind velocity, V in equation (1.1), may be written as the sum of mean and eddy flow components:

$$\vec{V} = \overline{\vec{V}} + \vec{V}' \quad (1.5)$$

As used here, $\overline{\vec{V}}$ is defined as the average wind computed over a volume characteristic of the mesh length to be used in the model. Since we assume sulfur dioxide to be photochemically inert, equation (1.1) may be written:

$$\frac{\partial C}{\partial t} + \nabla \cdot (\overline{\vec{V}} + \vec{V}') C = D \nabla^2 C + Q \quad (1.6)$$

The SO_2 concentration can also be considered the sum of deterministic (\bar{C}) and stochastic (C') components. Following the procedure delineated by Haltiner and Martin [1957], equation (1.6) is averaged to derive the equation for the mean concentration:

$$\frac{\partial \bar{C}}{\partial t} + \nabla \cdot \overline{\vec{V}C} + \nabla \cdot \overline{\vec{V}'C'} = D \nabla^2 \bar{C} + Q \quad (1.7)$$

Note that while the average of a fluctuation alone or of the product of a fluctuation with a mean vanishes, the covariance of two fluctuations is not negligible. The covariance term is the turbulent flux, which is assumed proportional to the gradient in \bar{C} (using the Prandtl Mixing Length principle; Haltiner and Martin, 1957, p. 245):

$$\nabla \cdot \overline{\vec{V}'C'} = -\nabla \cdot K \nabla \bar{C} \quad (1.8)$$

where K is the turbulent diffusion coefficient.

Observations have shown that diffusion due to molecular agitation is several orders of magnitude smaller than diffusion by turbulent eddies. Molecular diffusion can therefore be neglected, and if the initial flow surface is relatively smooth, equation (1.7) reduces to:

$$\frac{\partial \bar{C}}{\partial t} + \nabla \cdot (\overline{\vec{V}C}) = \nabla \cdot K \nabla \bar{C} + Q \quad (1.9)$$

Several further approximations are required in formulation of the Gaussian model. The zonal mean velocity, \bar{u} , is constant, and $\bar{v}=\bar{w}=0$. Since downstream advection is much greater than diffusion, diffusion along the plume axis is neglected ($K_x=0$). K_y and K_z are assumed constant. For an

elevated point source of height H over a perfectly reflecting terrain ($\partial C/\partial z \equiv 0$ at $z=0$), the solution to equation (1.9), with the above assumptions, is:

$$\bar{C} = \frac{Q}{2\pi\bar{u}\sigma_y\sigma_z} \exp(-y^2/2\sigma_y^2) \{ \exp(-[z-H]^2/2\sigma_z^2) + \exp(-[z+H]^2/2\sigma_z^2) \} \quad (1.10)$$

The quantities σ_y and σ_z are the standard deviations of particle distributions in the indicated directions and are functions of downwind distance and the statistical turbulence spectrum.

Equation (1.10) expresses the concentration of SO_2 at ground level as a function of the height of the source. Due to the buoyancy and exit velocity of the stack gases, however, the effective source height is really

$$H = H_s + \Delta H \quad (1.11)$$

where H_s is the stack height and ΔH is the rise of the plume after leaving the stack.

A number of formulae have been developed to describe plume rise, most based upon empirical relationships. From observation of more than 700 stacks Moses and Carson [1968] developed the following expression:

$$\Delta H = \frac{A w_s d_s}{\bar{u}} + \frac{B Q_h^{1/2}}{\bar{u}} \quad (1.12)$$

where A and B are constants which depend upon atmospheric stability. Plume rise figures used in this thesis are given in Table I.

TABLE I
PLUME RISE

WIND VELOCITY (M/SEC)	ATMOSPHERIC STABILITY CLASS			
	1 & 2 (unstable)	3 (slightly unstable)	4 (neutral)	5 (slightly stable)
1.	3206.51	2237.42	1479.85	1090.52
2.	1603.25	1118.71	739.92	545.26
3.	1068.86	745.81	493.28	363.51
4.	801.63	559.35	369.96	272.63
5.	641.30	447.48	295.97	218.10
6.	534.42	372.90	246.64	181.75
7.	458.07	319.63	211.41	155.79
8.	400.81	279.68	184.98	136.32
9.	356.28	248.60	164.43	121.17
10.	320.65	223.74	147.98	109.05
11.	291.50	203.40	134.53	99.14
12.	267.21	186.45	123.32	90.88
13.	246.65	172.11	113.83	83.89
14.	229.04	159.82	105.70	77.89
15.	213.77	149.16	98.66	72.70
16.	200.41	139.84	92.49	68.16
17.	188.62	131.61	87.05	64.15
18.	178.14	124.30	82.21	60.58
19.	168.76	117.76	77.89	57.40
20.	160.33	111.87	73.99	54.53

C. AN ALTERNATE MODEL

As discussed earlier, the complex and irregular nature of turbulent boundary layer flow within the coastal airshed precludes the use of exact or measured meteorological data to describe diffusion. Nonetheless there exists the need to statistically parameterize this turbulence and include such considerations in pollutant dispersal models. The assumption of homogeneous, isotropic flow which yields the Gaussian solution also eliminates flow boundaries from consideration. Wind velocity is required to be constant, a dangerous oversimplification.

Obviously, the need exists for a multipurpose diffusion model capable of handling variable meteorological parameters. Since present knowledge is not adequate to permit a rigorous interpretation of turbulent transfer processes, the optimum approach should consider each aspect of the problem separately. The best approximation derived for each phase can then be incorporated in the model.

Returning to equation (1.9), let horizontal diffusion be isotropic ($K_x = K_y = K_H$). The further assumption that K_H is constant in space and time is poor, since in fact the eddy diffusivity depends on both transport time and height; however, this simplification can later be rectified. Thus equation (1.9) can be written

$$\frac{\partial \bar{C}}{\partial t} = -\bar{\vec{V}}_H \cdot \nabla_H \bar{C} + K_H \nabla_H^2 \bar{C} + \frac{\partial}{\partial z} K_z \frac{\partial \bar{C}}{\partial z} + Q \quad (1.13)$$

where the vertical advection, $\bar{w} \frac{\partial \bar{C}}{\partial z}$, has been omitted as a first approximation (since $\bar{w} \approx 0$ near the ground except for terrain effects).

1. Boundary Conditions

The boundary conditions are assumed to be:

$$\nabla \bar{C} = 0 \text{ at } x=y=z=0, \ x=x_{\max}, \ y=y_{\max}, \ z=Z \quad (1.14)$$

where Z = inversion height. Exact lateral boundary conditions cannot be formulated, but as Shir and Shieh [1973] noted, the lack of well-posed boundary conditions does not cause serious problems.

2. Formulation of Numerical Model

The accuracy of an analytical solution to equation (1.13) is restricted by the nonlinear nature of pollutant advection. In like manner, finite difference approximations to the advective term can introduce phase and amplitude errors in the numerical model. Simple upstream difference schemes, for example, produce a false dispersive effect which would make any results meaningless. Solutions obtained using centered-difference forms of the governing equations are subject to stability limitations on the size of the time-step relative to the spatial mesh size of the model. These stability restrictions can lower computational efficiency by imposing a smaller timestep than would otherwise be desirable. Thus a key disadvantage of explicit finite difference approximations to equation (1.13) is that the maximum time-step is fixed by the spatial grid distance rather than by the rate of change of the physical variables involved.

3. Implicit Methods

The unconditional stability of implicit methods makes them particularly desirable from a meteorological standpoint. Until recently, however, the implicit solution of large-matrix partial differential equations was accomplished almost exclusively by iterative relaxation techniques. In pure form, such as with Liebmann Overrelaxation, these methods require large amounts of core storage and do not take advantage of the zero structure of solution matrices.

To remove these objections, a noniterative class of methods known as alternating direction implicit (ADI) has been developed. Douglas [1962] modified the Crank-Nicholson equation to yield a three-step ADI scheme for the solution of mildly-nonlinear, three-dimensional parabolic and elliptic problems. The original alternating direction concept has since been expanded and generalized; a discussion of various techniques is given by Mitchell [1969].

Following Douglas' technique, the difference equations for equation (1.13) are:

X-SWEEP:

$$\left[\frac{1}{\Delta t} + \frac{\bar{u}}{2} \hat{\nabla}_x - \frac{K_H}{2} \Delta_x^2 \right] C_{ijk}^{n+1/3} = \left[\frac{1}{\Delta t} + \frac{K_H}{2} \Delta_x^2 + \hat{\nabla}_z K_z \hat{\nabla}_z - \frac{\bar{u}}{2} \hat{\nabla}_x - \bar{v} \hat{\nabla}_y \right] C_{ijk}^n + Q_{0,0,H}$$

Y-SWEEP:

$$\left[\frac{1}{\Delta t} + \frac{\bar{v}}{2} \hat{\nabla}_y - \frac{K_H}{2} \Delta_y^2 \right] C^{n+2/3} = \left(\frac{1}{\Delta t} \right) C^{n+1/3} + \left[\frac{K_H}{2} \Delta_y^2 - \frac{\bar{v}}{2} \hat{\nabla}_y \right] C^n \quad (1.15)$$

Z-SWEEP:

$$[\frac{1}{\Delta t} - \frac{1}{2} \hat{\nabla}_z K_z \hat{\nabla}_z] C^{n+1} = (\frac{1}{\Delta t}) C^{n+2/3} + [\frac{1}{2} \hat{\nabla}_z K_z \hat{\nabla}_z] C^n$$

As used here, the operators $\hat{\nabla}$ and Δ^2 apply at the point i, j, k . Space subscripting is eliminated to simplify notation. Forms of the finite-difference operators used are:

$$\hat{\nabla}_{x(y,z)} C_{ijk}^n = \frac{C_{i+1,j,k}^n - C_{i-1,j,k}^n}{2\Delta x} = \left. \frac{\partial C}{\partial x} \right|_{i,j,k}^n + O(\Delta x)^2 \quad (1.16)$$

$$\Delta_{x(y,z)}^2 C_{ijk}^n = \frac{C_{i+1,j,k}^n - 2C_{ijk}^n + C_{i-1,j,k}^n}{(\Delta x)^2} = \left. \frac{\partial^2 C}{\partial x^2} \right|_{i,j,k}^n + O(\Delta x)^2$$

When applied at successive grid points, equation (1.15) generates a tridiagonal system of equations for C^{n+1} . The formal temporal accuracy of the solution is increased by the use of Crank-Nicholson centering about $t^{n+1/2}$ (i.e. by averaging terms on the RHS of equation (1.13) between the n th and $(n+1)$ st levels).

V. MODEL APPLICATION

A. SOURCE DATA

The intensity of stack SO₂ discharges and the physical design of the hypothetical power plant used in both thesis models are taken directly from data provided by Mr. R. C. Puckett of Pacific Gas and Electric Co., Moss Landing. These data are summarized in Table II.

B. GAUSSIAN MODEL

1. Grid

The southern half of Monterey Bay is divided into a receptor grid comprising 875 points: 25 points spaced one kilometer apart oriented east-west, by 35 points one km apart oriented north-south. The location of the power plant source is fixed at X=0.0, Y=0.0 and is the northwesternmost grid point.

2. Meteorological Data

a. Wind Field

For initial runs the surface wind direction is assumed constant at 315°. Wind velocity is varied from one mps to twenty mps in increments of one mps.

Standard procedure, in estimating the diffusion of an effluent at a downwind distance of more than a few kilometers, is to assume a constant wind field. The center-line of the plume is then assumed to move in a straight line following the same trajectory computed at the source location.

TABLE II

THEORETICAL POWER PLANT SPECIFICATIONS

Location of Power Plant

X-COORD	Y-COORD
0.0 M	0.0 M

Fuel: Oil (Primary) and Nat. Gas (as available)

Actual Stack Height: 155.0 M

Inside Stack Diameter: 6.0 M

Stack Gas Exit Velocity: 20 M/SEC

Stack Gas Temperature: 425 Deg K

Stack Gas Constituents (in percent):

NO_x: 72.1

SO₂: 0.3

CO₂: 13.7

Particulates: xx.x

Hydrocarbons: xx.x

Total Volume of Stack Gas Discharge: 7.01×10^7 CU FT/HR

Waste Heat Discharge: 1.0×10^9 BTU/HR

SO₂ Source Intensity (est): 30 GM/SEC

This simple procedure is particularly inadequate in the coastal zone because of the complicated effects of the land-sea boundary and topographic influences.

b. Atmospheric Stability and Dispersion Coefficients

The standard deviations, σ_y and σ_z , of plume concentration distribution in the horizontal and vertical vary with the turbulent structure of the marine layer. The dispersion coefficient curves from Turner [1969] are used in the Gaussian model. Turner based his values of these parameters upon stability estimates of the lowest few hundred meters of the atmosphere, over "relatively open country". Stability is in turn determined by wind speed and insolation. Five classes are delineated (Table III), with lapse rates approaching neutral more closely for greater wind speeds.

As previously shown, the thermal structure of the marine layer produces good vertical diffusion below the elevated inversion with virtually zero diffusion through the base of the stable layer. In a study of the same Moss Landing plant, Kraft [1971] noted the relative insensitivity of the atmosphere to the large quantities of waste heat discharged from the stacks. Thus the thesis model treats the inversion layer as a physical barrier to pollutant diffusion and ignores any local "heat island" effect of the plant.

TABLE III
STABILITY CLASSIFICATION

WIND SPEED (mps)	INSOLATION			
	3 (strong)	2 (moderate)	1 (weak)	0 (night)
<2	1	2	2	5
2-3	2	2	3	5
4-5	2	3	3	4
6	3	4	4	4
>6	3	4	4	4

[after Turner, 1969]

C. ALTERNATING DIRECTION IMPLICIT MODEL

1. Grid and Timestep

In order to provide for a more detailed analysis and to prevent eddy-scale phenomena from being smoothed, the horizontal mesh length for the ADI model was reduced to 0.5 km. A 60-meter vertical spacing is used, dividing the marine layer (600 m thick) into ten equal sublayers. The horizontal grid is oriented north-south (30 by 30 points). The power plant is located at $X=0.0$, $Y=7.5$ km, $Z=300$ m.

Selection of a timestep represents a critical decision. The most important factor to be considered in determining the step size is the time scale of atmospheric motions being described. Holland [1967] categorized the following time and length scales of turbulent atmospheric motion:

- 1) inertial turbulence: <10 sec, <50 m
- 2) mechanical turbulence: 10-100 sec, 50-500 m
- 3) thermal turbulence: 100-1000 sec, 500-5000 m.

The mixing time for a typical turbulent marine layer has been described by Shieh (personal communication) as about ten minutes and by Lamb (personal communication) as 15 minutes. Thus to parameterize the process of diffusion on a turbulent scale, a time increment of 30 seconds has been used.

2. Meteorological Conditions

a. Wind Field

For the ADI model, the wind vector

$$\vec{V}_{ij} = \bar{u}_{ij}(x,y) + \bar{v}_{ij}(x,y)$$

is required at all grid points for each sweep. As with the Gaussian method, a constant wind field is input, with all levels normalized to the input field (selected as 10 m). For ease of computation the u-component of the wind is defined such that flow is along the axis of the "average" plume. Since total displacement over total travel time is a measure of the mean velocity, the displacement timescale is a natural one over which to define the average concentration expressed by equation (1.13). Thus the velocity components causing diffusion are deviations definable by statistical moments such as diffusion coefficients.

Since wind data for specific levels within the marine layer are not available, the direction of horizontal wind flow is assumed constant with height. This assumption neglects the effects of directional shear; unfortunately the detail of available meteorological observations is not sufficient to correct this omission.

Vertical wind profiles are assumed to be of power law form:

$$\vec{V}_k = \vec{V}_n (z_k/z_n)^p \quad (2.1)$$

where $\vec{V}_n = \vec{V}(10m)$ and $z_n = 10m$. The power coefficient, p , is varied from 0.1 to 0.4 according to stability class. Figure 3 shows vertical wind profiles (normalized to the ten meter level) for each stability category.

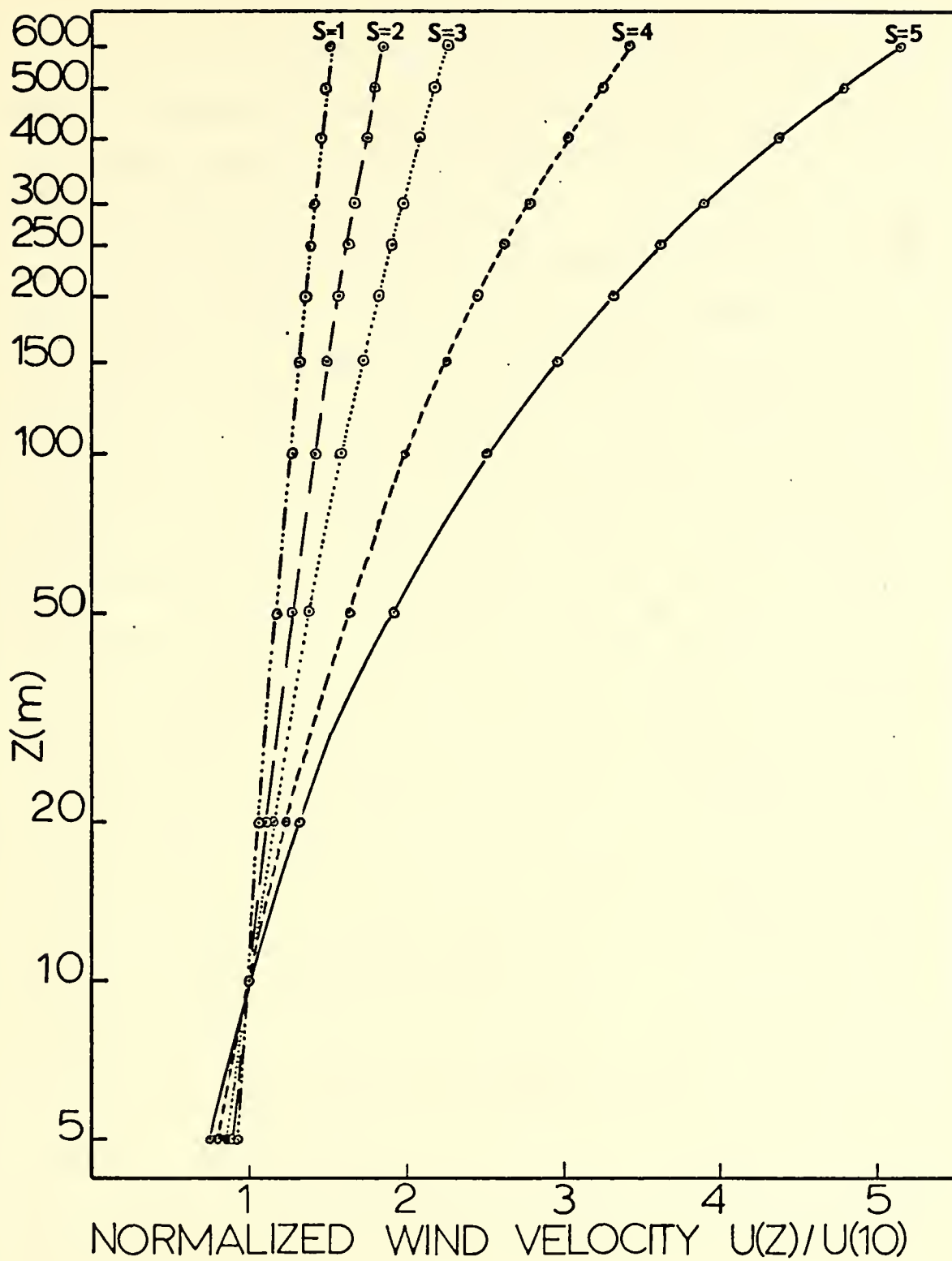


FIGURE 3 ADI VELOCITY PROFILES

b. Atmospheric Stability

In previous discussion the rate of diffusion of airborne pollutants has been attributed to the scale and intensity of atmospheric turbulence. This turbulence is directly related to stability.

Classifications of atmospheric stability such as the Pasquill-Gifford scheme used in the Gaussian model do not satisfactorily describe the topographic influences so important in generating turbulence. The Richardson number, Ri and the Monin-Obukhov length, L are frequently-used stability functions in boundary-layer theory. Unfortunately, both parameters depend upon the accuracy of input vertical temperature gradients. Recently, however, Golder [1972] related the Pasquill-Gifford stability classes to the Monin-Obukhov length, incorporating surface roughness (z_0) and eliminating the requirement for vertical temperature profiles. The Monin-Obukhov stability length is more convenient to use in the formulation of diffusion coefficients since it can be considered independent of altitude in the boundary layer. The Golder formula is

$$\frac{1}{L} = (\pm) [0.216586 \cdot \ln(1.2 + \frac{10}{z_0})]^2 \cdot 10^{f(s)} \quad (2.2)$$

where $f(s) = \frac{-4.0}{(1+1.3|s|^{0.85})}$, s = stability class.

The sign of s determines the sign of the RHS of (2.2); negative values are unstable, positive values stable. Golder's formula is applied in the ADI model using a value of 1.5 meters for z_0 .

c. Diffusion Coefficients

Calculation of eddy diffusivities is at best a guessing game, since data are sparse and estimates of both K_H and K_z vary in recent literature by at least an order of magnitude. These parameters are known to depend upon altitude, wind velocity, atmospheric stability, surface roughness and travel time but the relationship in each case is poorly established.

Horizontal shearing stress has already been assumed constant. Travel time thus is probably the most important factor in determining the coefficient of horizontal eddy diffusion, K_H . As a pollutant cloud spreads downwind, the frequency of the turbulent elements most effective in dispersing particles decreases, so that the magnitude of eddy exchange increases. In order to parameterize this change, K_H is initially set at $10^2 \text{m}^2/\text{sec}$ (a frequently-quoted value), and is then incremented within the time loop by $100 \text{m}^2/\text{sec}$ at successive downstream grid points. When the value $K_H = 10^3 \text{m}^2/\text{sec}$ is reached incrementation stops; K_H is held constant beyond that time.

The vertical distribution of K_z under neutral conditions has been given by Shir and Shieh [1973] as

$$K_z = u_* l \quad (2.3)$$

where $l = k_0 z \exp(-4 z/H)$,

u_* = friction velocity,

k_0 = von Karman constant = 0.41,

H = depth of boundary layer (taken as 100m).

For non-neutral conditions,

$$K_z = K_s (1/l_s) \quad (2.4)$$

where the subscript s denotes values derived from the input "surface" wind velocity field, and the Monin-Obukhov length computed above. Luers [1973] describes the mean wind for the surface boundary layer (corresponding to \vec{V}_{ij}) as

$$\bar{u} = \frac{u^*}{k_0} \left[\ln \left(\frac{z+z_0}{z} \right) + \psi \left(\frac{z}{L} \right) \right] \quad (2.5)$$

from which u^* can be computed. For neutral stability, $s=0$, $\psi(z/L)=0$, but for unstable conditions, $s<0$,

$$\psi \left(\frac{z}{L} \right) = \int_{z_0/L}^{z/L} \frac{L}{z^2} \left[1 - \left(1 - 18 \frac{z}{L} \right)^{-1/4} \right] d \left(\frac{z}{L} \right) \quad (2.6)$$

For stable conditions, $s>0$,

$$\psi \left(\frac{z}{L} \right) = 5.2 \left(\frac{z}{L} \right).$$

Using the value computed for u_* , assuming the mean wind level is 10m, $K_s=K_z(z=10m)$ is then calculated and extrapolated for (0-100m). Above 100m the change in K_z is assumed to be negligible and $K_z=K_z(z=100m)$. The normalized profiles for K_z under neutral and slightly unstable conditions are displayed in Figure 4.

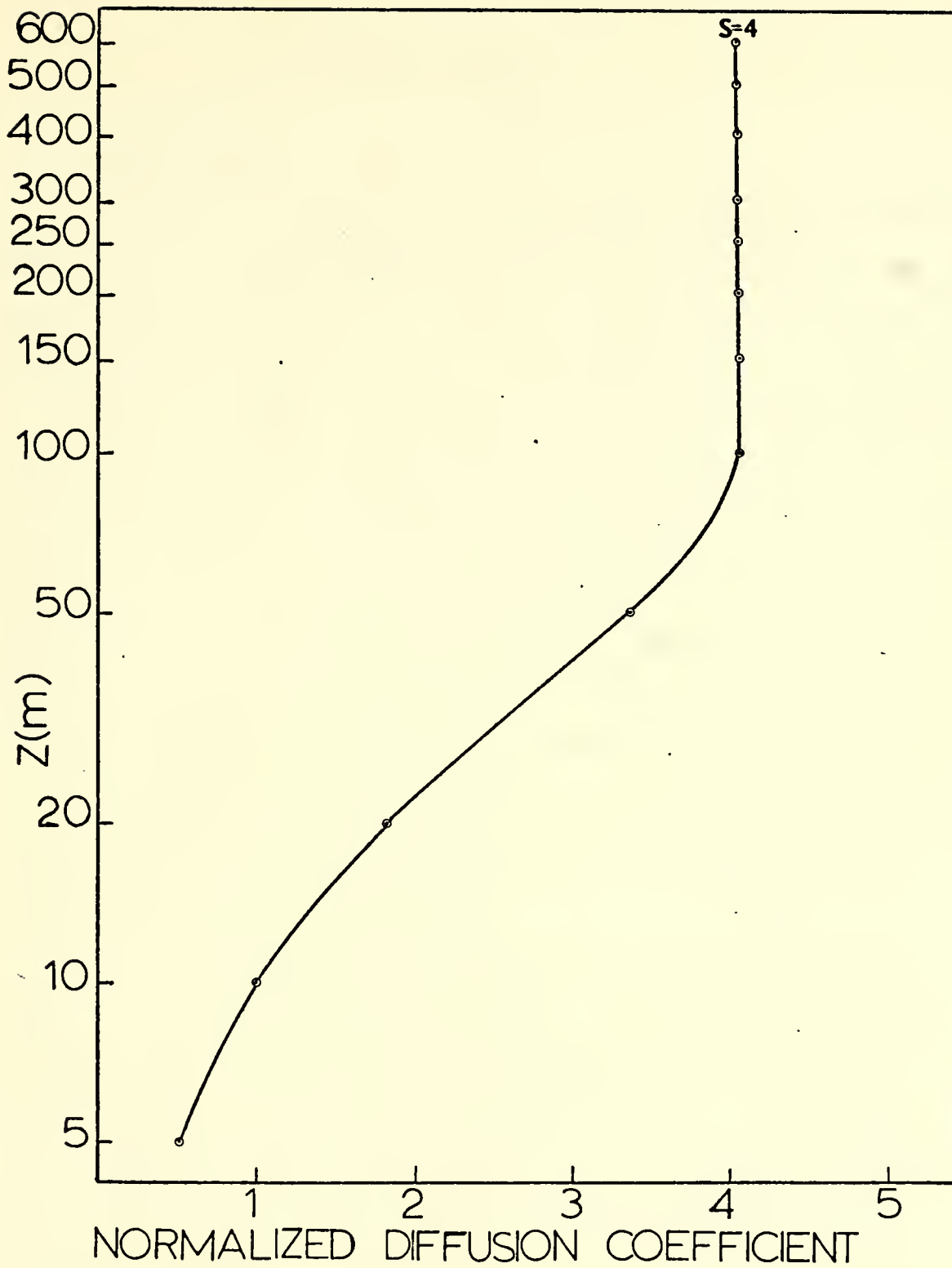


FIGURE 4 ADI DIFFUSION COEFFICIENTS

VI. RESULTS

A. GAUSSIAN MODEL

Pollutant concentrations calculated by the Gaussian diffusion program under various meteorological conditions are described by Figures 5-9. Numerical values given are peak ground-level concentrations in micrograms per cu. meter.

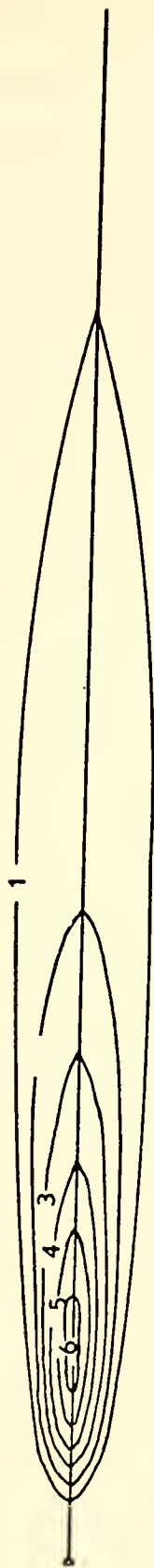
Figure 5 compares individual profiles for stability conditions ranging from neutral ($s=4$) to moderately unstable ($s=2$). Wind speed and marine layer thickness for the three sets of curves are the same. Based upon an initial source intensity of 30 gm/sec, computed surface concentrations are within a fairly narrow range: from $2.3\mu\text{gm-cu.m}^{-1}$ for $s=4$ to $11.9\mu\text{gm-cu.m}^{-1}$ for $s=2$. However, downwind distance to the peak concentration varies by an order of magnitude, describing the response of dispersion rates to increased thermal turbulence in the atmosphere.

Figure 6 relates typical profiles of cases for which wind and stability are held constant, varying only the inversion height. Since the peak surface concentration as described by equation (1.10) is not related to layer thickness, the SO_2 ground-level maxima are identical, as is distance to the peak value. Downstream from the point of maximum concentration the reduction of contaminant is much slower for the low-inversion case due to trapping in the marine layer.



FIGURE 5 DOWNWIND SO₂ CONCENTRATION
AS A FUNCTION OF STABILITY

250m MARINE LAYER



1200m MARINE LAYER

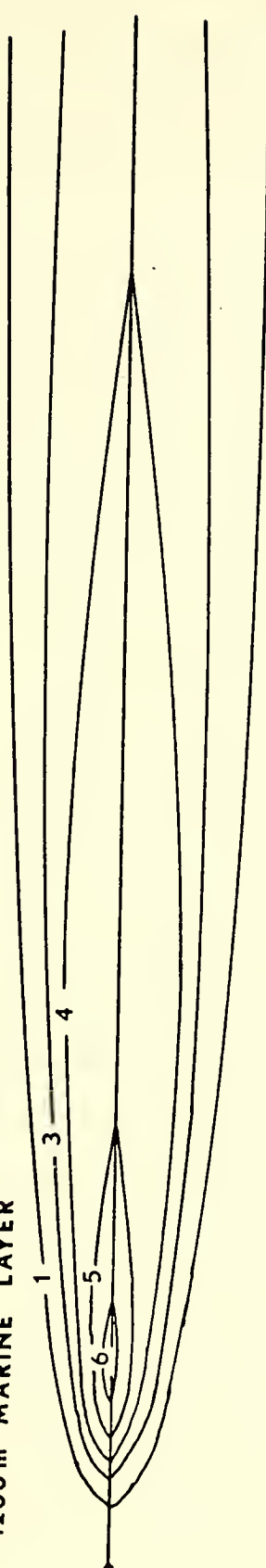


FIGURE 6 DOWNWIND SO₂ CONCENTRATION
AS A FUNCTION OF MARINE LAYER DEPTH

Variation of wind strength affects ground-level values as shown in Figure 7. Distance to peak concentration varies inversely with wind speed; however, the maximum intensity is greater for the intermediate wind speed (4 mps) than for either the 2mps or 16 mps cases.

Figures 8 and 9 are composites of all cases studied. In Figure 8, the maximum ground-level concentration is plotted as a function of wind speed and stability class. For winds stronger than 5 mps concentrations depend primarily upon stability; below 5 mps there is a pronounced increase in dependence upon wind speed, and a reversal in the trend of reduced peak concentrations with increasing distance from the source. For the stable cases ($s=5$), peak surface values continued to increase to the edge of the grid but were significantly lower than values obtained for neutral or unstable conditions.

Figure 9 shows downwind distance along the plume axis to the peak ground-level concentration, again as a function of stability and wind speed. Notice that the dependence upon stability class is almost total for stronger winds but that wind speed again becomes significant below about 5 mps.

B. ADI MODEL

Figures 10-13 show results obtained from the ADI model. Note that the basic purpose of these computations is to examine the capabilities of the alternating direction method for the implicit solution to three-dimensional flow equations.

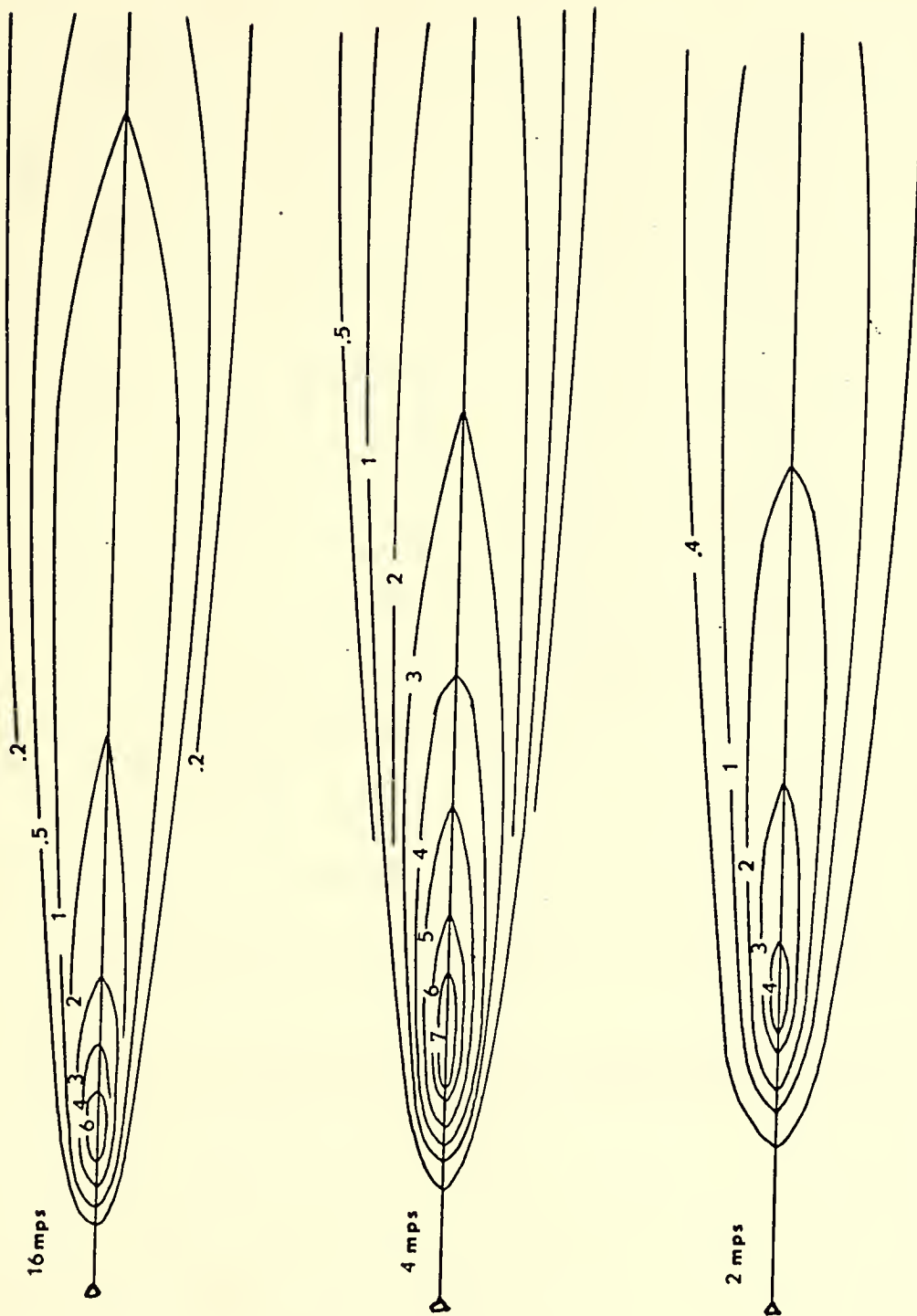
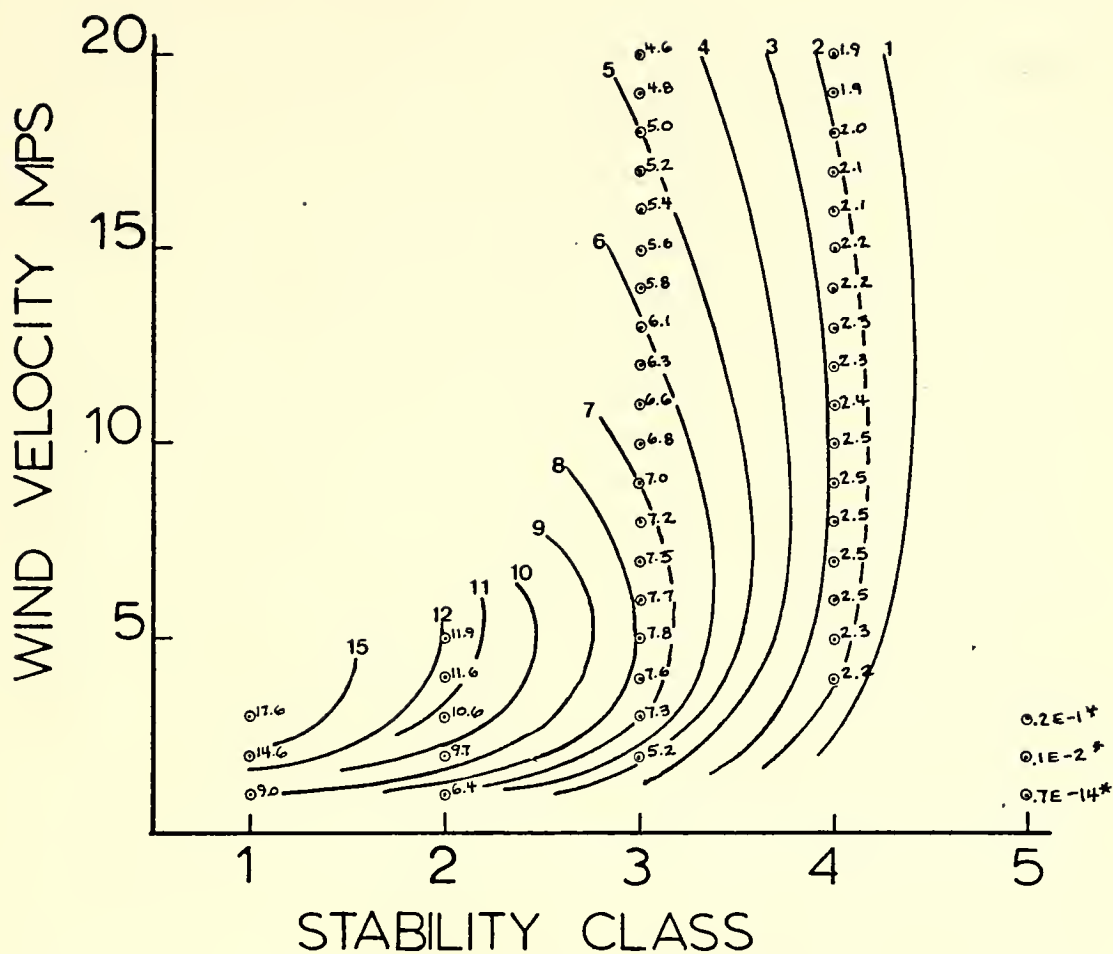
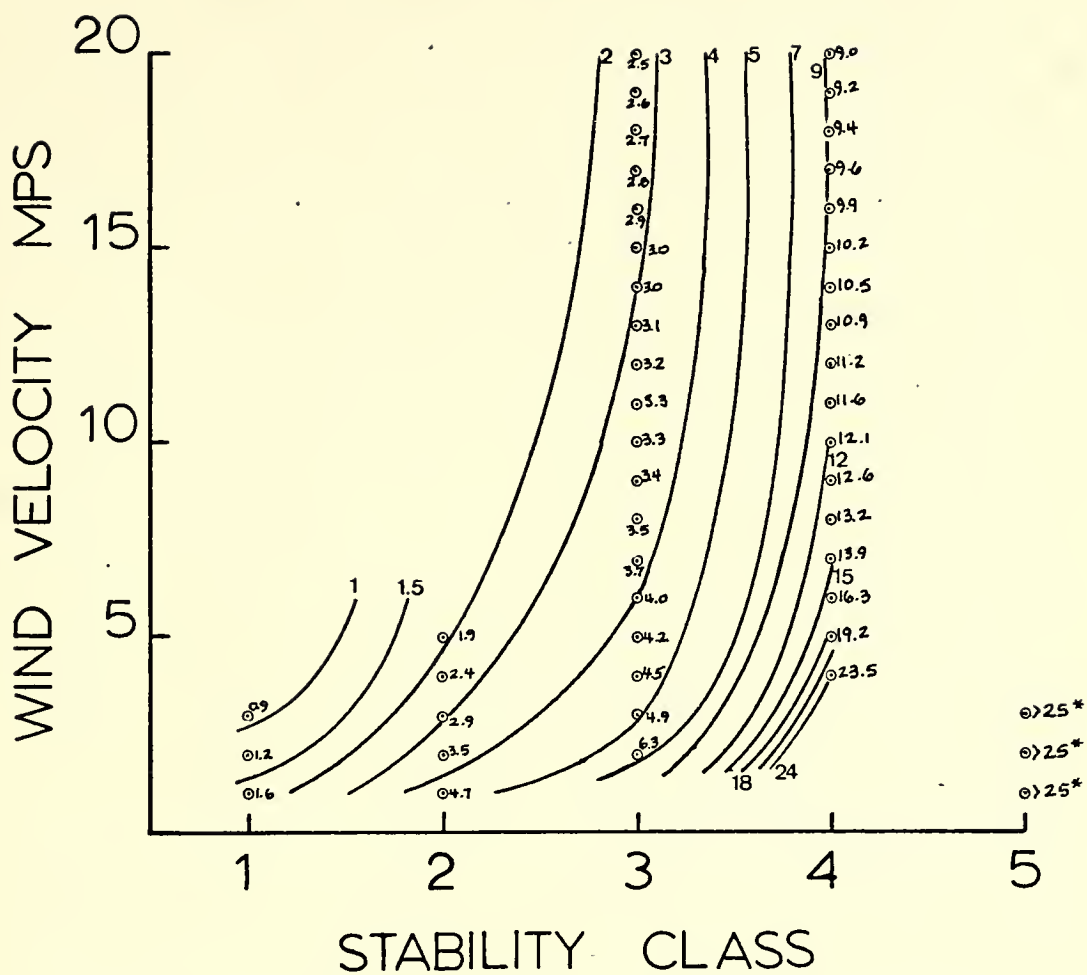


FIGURE 7 DOWNWIND SO₂ CONCENTRATION
AS A FUNCTION OF WIND VELOCITY



*values at 25 km, concentration still increasing

FIGURE 8 PEAK GROUND-LEVEL CONCENTRATION: $\mu\text{gm}/\text{m}^3$



*values at 25 km, concentration still increasing

FIGURE 9 DISTANCE TO PEAK GROUND-LEVEL CONCENTRATION FROM SOURCE: km.

Thus, concentration values are not to be compared analytically with the Gaussian results to judge the accuracy of either method.

In the course of developing the numerical scheme, solutions were developed for the case of Fickian diffusion, with $K_x = K_y = \text{constant}$ and $K_z = \text{constant}$. A vertical, axial-plane profile describes these results in the marine layer (Figure 10). The solution is given for a short-term (30 minute) calculation using a 30-second timestep. Concentrations fall off rapidly downstream and show strong vertical gradients. Defining the plume boundary as the surface at which the pollutant concentration is ten percent of the axial value on the same crosswind plane, the plume travels approximately five km downstream before ground contamination occurs.

Figures 11-13 describe the effects of varying stability and wind velocity on dispersion, plotted on the axial vertical plane. These calculations include the horizontal and vertical diffusion coefficients discussed in MODEL INPUT. With reduced atmospheric stability, plume axial concentration decreases more rapidly, but ground-level contamination occurs earlier. At a wind speed of 10 mps, the plume edge reaches the surface about 3.5 km downstream under slightly unstable conditions but travels nearly 11 km before grounding under neutral stability. Reducing wind speed slows the decrease in axial concentration but increases the distance to the surface contamination point.

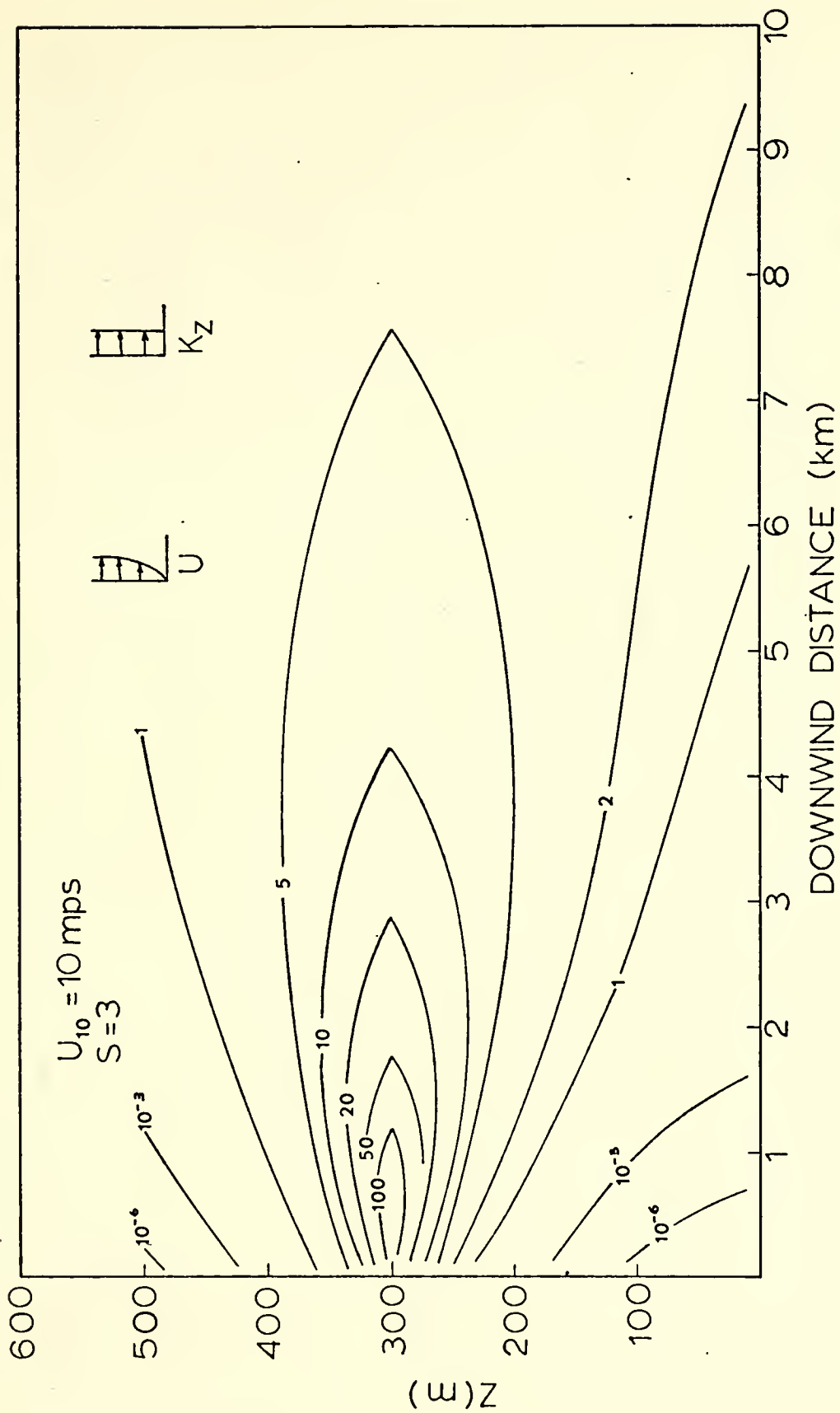


FIGURE 10

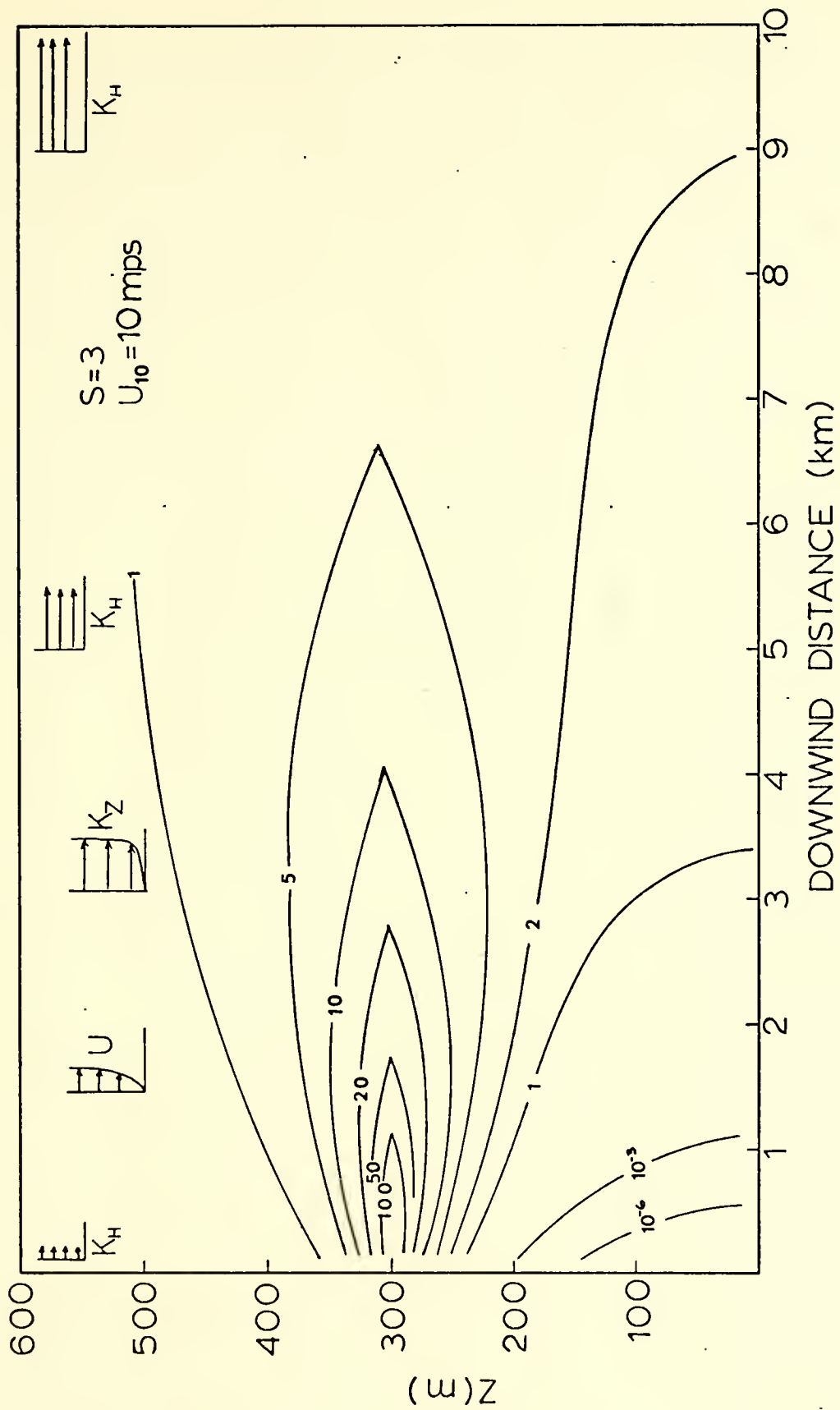


FIGURE 11

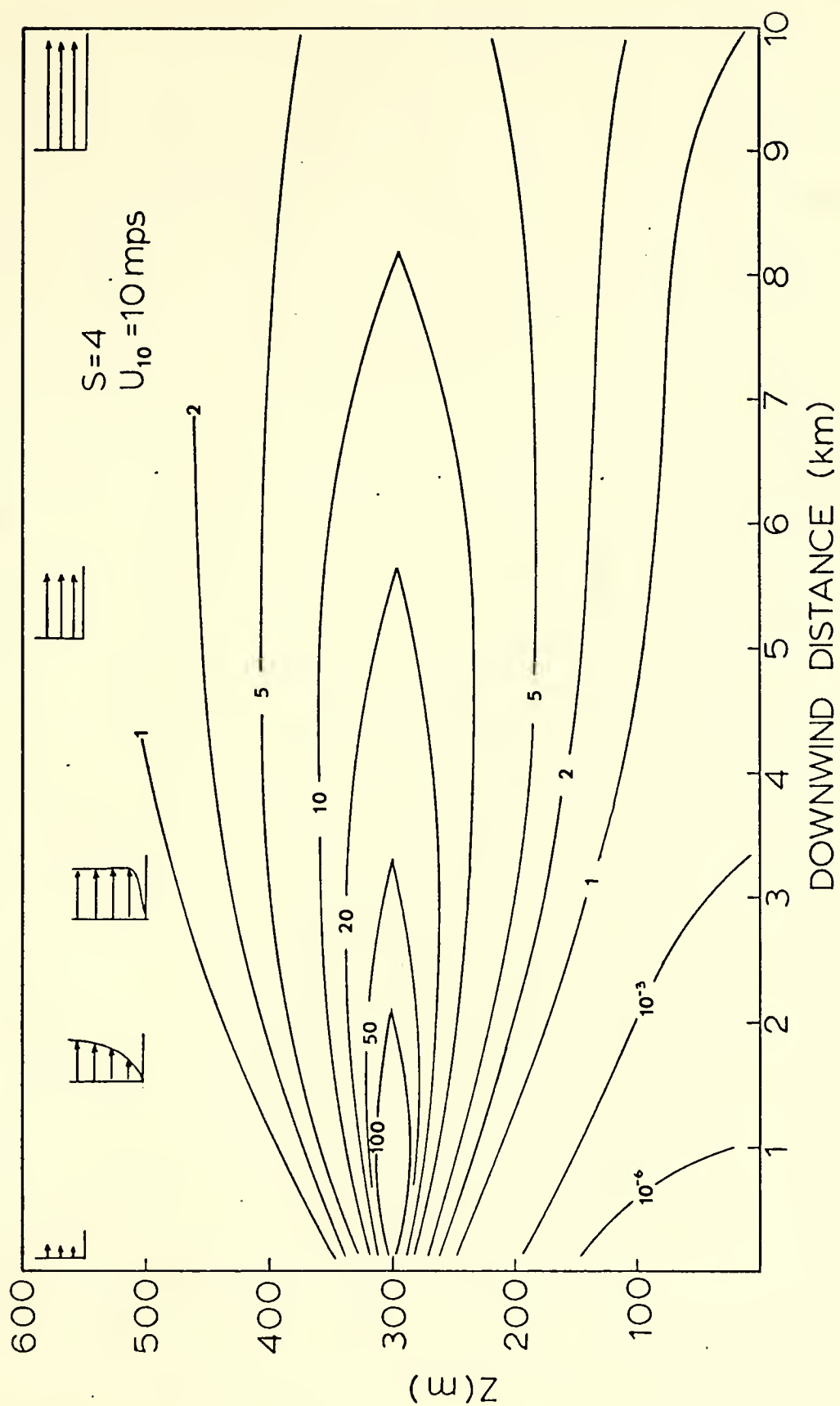


FIGURE 12

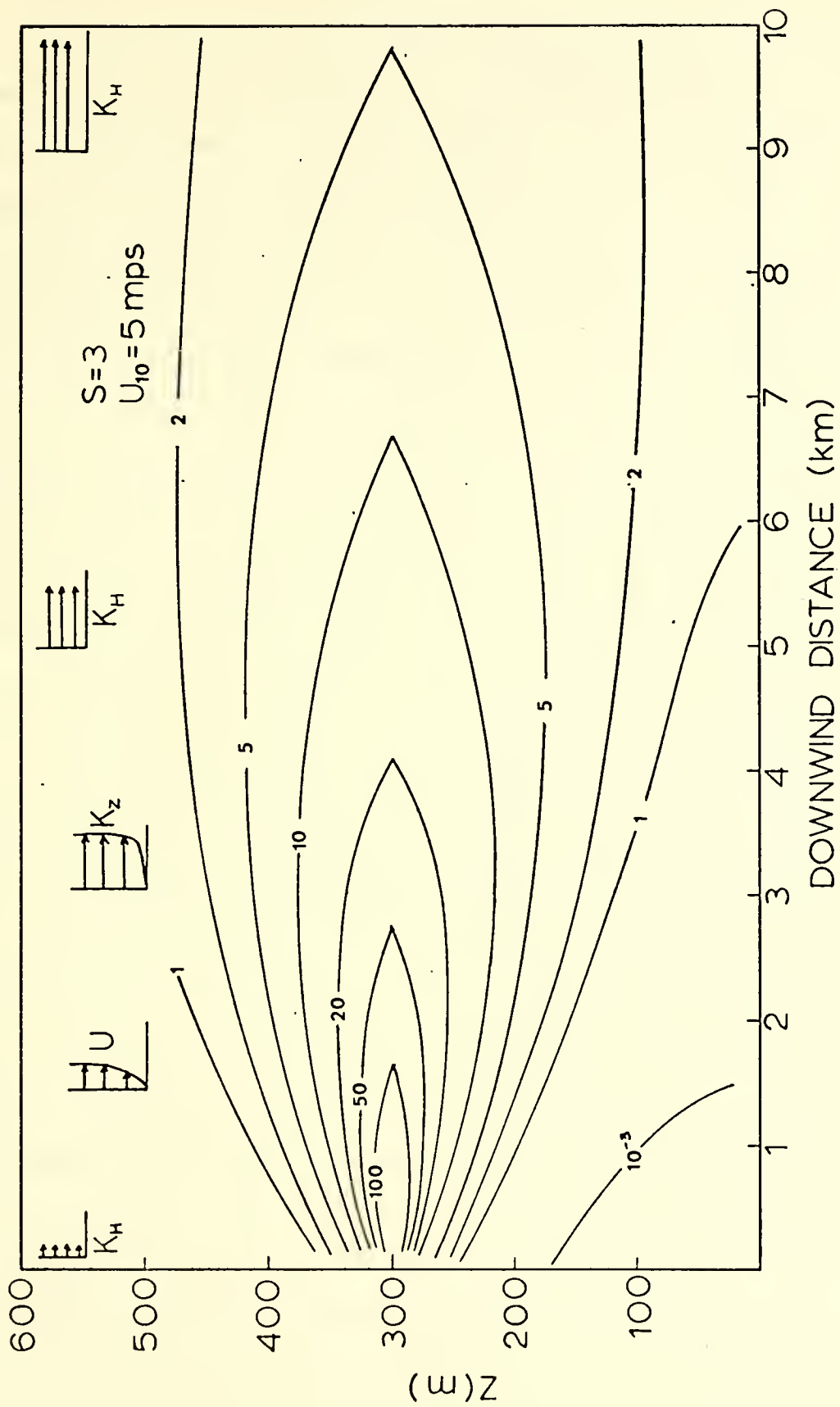


FIGURE 13

C. DISCUSSION OF RESULTS

The results of both models can be interpreted to yield some important generalizations concerning pollutant transport and diffusion in the atmosphere. The Gaussian model predicts statistical patterns of concentration, while the stochastic model deals with the probabilistic nature of diffusion. Both approaches have relevance in the atmosphere.

From the patterns described by Figures 5-9 it is apparent that peak ground concentrations predicted for winds in excess of five mps show much less dependence upon the actual wind speed than do values obtained for winds less than five mps. This difference can be attributed in part to the predominance of thermal turbulence at low wind speeds. Since the stability classification used in this study is derived as a function of wind velocity, results are difficult to interpret, but the fact seems well-established that weaker winds are more affected by thermal instability in the air. For strong winds the velocity profile must be dominated by the effects of mechanical turbulence, since only neutral or slightly unstable conditions are permitted at wind speeds in excess of five mps. This observation correlates well with the observations of Panofsky [1964] who found the high-frequency end of the turbulent velocity spectrum to be independent of stability, and the low-frequency range strongly influenced by stability. In the case of low wind speeds, the simple power law formula used to define the wind field for the ADI model would therefore cease to be valid due to

the downwind dominance of thermally-driven turbulence in the lower atmosphere.

In addition, under conditions of light wind the effective stack height is greatly increased by plume rise, frequently carrying the stack effluent through the inversion layer. Pollution hazards under such conditions are therefore not likely to be very serious. When an exceptionally strong inversion exists under stagnating anticyclonic flow, however, the potential for significant atmospheric contamination is much greater.

Both methods predict more rapid ground-level contamination as wind velocity increases. For lower wind speeds the Gaussian plume is released from a much greater effective height and the downwind dislocation of surface maxima is the expected result. However, the plume rise correction is not applied to the ADI model; thus the inverse relationship between wind speed and ground contamination distance must be attributed to more effective vertical diffusion, accomplished by the increase in K_z due to a larger u_* in equation (2.1) (see Figures 11 and 12).

If the size of the largest eddies responsible for spreading the plume vertically is considered to be approximately the same as the crosswind plume dimensions one sees that mechanical turbulence can easily accomplish the necessary diffusion within the scale depth of the marine layer. Horizontal mixing is a much slower process, involving time-scales of hours or days until total equilibrium of concentration is established. Thus the turbulent response of the

boundary layer to topographic obstacles and other surface features will significantly alter vertical diffusion rates but will average out in horizontal dispersal.

Concentration patterns produced by varying atmospheric stability (Figures 5, 8-9, 11-12) reveal the significance of vertical mixing determined by the marine layer thermal structure. Both models effected more rapid vertical diffusion in less stable air; the Gaussian model by means of larger σ_z values, the ADI model by means of increased turbulence as represented by the diffusion coefficient. These effects induce more rapid vertical diffusion, so that surface contamination at fairly high levels occurs within a few kilometers downstream of the source. Under stable conditions the damping of turbulence is so strong that flow is nearly laminar, trapping the pollutant in a duct near the effective height of injection and allowing essentially no pollutant ground deposition. Neutrally-stable marine layers yield results in between, with low-intensity surface pollution occurring at great distances downwind.

Time restrictions precluded tuning the ADI model for study of marine layer depths other than 600 meters. However, from the results of the Gaussian model (Figure 6) it is evident that significant pollution episodes are far less likely when the vertical extent of the marine layer is great.

VII. CONCLUSIONS AND RECOMMENDATIONS FOR FUTURE STUDY

The results of this thesis, though admittedly preliminary, permit some broad conclusions regarding the general role of the atmosphere in dispersing contaminants. Non-reactive constituents and small particulates emitted into the atmosphere drift with the prevailing airstream, spreading progressively in both vertical and horizontal directions until they are removed by various natural processes (not considered in this study). The pollutants tend to be distributed initially over a volume of air directly proportional to the wind speed, with simultaneous dilution by turbulent and convective motions which disturb the mean flow. Downwind from a continuous emission, correlation of source data and various parameters of the idealized atmosphere shows peak concentrations to be directly proportional to rate of emission and inversely related to wind velocity and rate of diffusion.

Effective emission height is shown to be a significant characteristic determining downstream concentrations. At greater elevations, pollutants must travel farther with correspondingly greater vertical and crosswind dilution before ground-level contamination occurs. Since the effective source elevation is largely determined by wind velocity, the latter (along with inversion height, which is wind speed-related) is the most critical factor controlling pollution. In particular, under conditions of light wind when advection

is reduced and diffusion is uncertain, estimates of the dispersive action of the atmosphere are not reliable. Strong winds produce concentration patterns which can be more dependably estimated from statistical fluid properties.

The dependence of eddy diffusion rates upon atmospheric thermal stability is well-established and has been reaffirmed by results presented in this thesis. A first objective for further study should therefore be the definition of a stability parameter which is a continuous function of marine layer stability. If accurate predictions are desired, eddy exchange coefficients must be computed from stability curves based on real-time, detailed thermal data (usually not routinely available).

With specific regard to the downstream variation of eddy diffusion, literature is virtually nonexistent. The increased diffusive effectiveness of progressively larger turbulence elements acting upon a cloud or plume moving downwind seems obvious. The nature of such variance (treated linearly in this study) is not established and appears worthy of further evaluation.

Any complete study of atmospheric diffusion in the coastal zone should consider the rapid changes in marine layer thermal structure occurring as a result of the temperature and terrain differences between land and water. Future research applied specifically to the Monterey area should study the effects of the land-sea breeze thermal circulation on pollutant dispersal. Under conditions of

onshore flow the thermal irregularities of underlying terrain will introduce serious complications into the analysis of diffusion; thus the effects of elevation, ground cover and moisture should be considered.

Reasons for the preference of Gaussian dispersal models over more sophisticated schemes have already been discussed. The statistical method used in this study computes a solution at 875 grid points for each of 20 wind speeds under four categories of insolation in less than eight seconds, requiring 49K bytes of core storage. Concentrations calculated by the time-dependent ADI model require nearly 300 seconds and more than 170K for each wind speed and stability class (9900 grid points). Although no verifying data can be applied in either case, for short-term calculations the use of numerical simulation schemes is difficult to justify in light of the above cost comparisons. On the other hand, the terrific potential of time-dependent models to incorporate the effects of an observed, spatially- and temporally-variable wind field adjusted for topographic influences may outweigh considerations of computational economy.

The analysis of contaminant dispersal in the marine layer can provide valuable insight into the dynamics of that region. The history of an inert pollutant particle depends to a very great extent upon the turbulent properties of the near-surface atmospheric flow. Detailed wind observations and thermal profiles are rarely plentiful enough to reveal the strongly topography-dependent characteristics of the

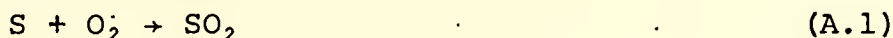
turbulence theory. Observations of the transport of atmospheric contaminants such as sulfur dioxide may be used qualitatively to extend the available data base for the analysis of boundary-layer phenomena.

APPENDIX A

ATMOSPHERIC SULFUR DIOXIDE: GENERAL CONSIDERATIONS

A. SOURCES

Combustion of sulfur-containing hydrocarbon fuels is the only significant cause of sulfur dioxide pollution in the atmosphere. Coal-burning power and industrial plants and the internal combustion engine are the major contributors. The governing reaction is



B. ATMOSPHERIC REACTIVITY

The oxidation of SO_2 in a mixture of gases is slow, but the rate increases in sunlight and in the presence of NO_2 , oxidants, and metallic oxides which act as catalysts. The reactions are:



C. EFFECTS

1. Damage to Inorganic Materials

Many substances suffer serious corrosive damage when exposed to sulfuric acid vapor, which is the secondary pollutant derived from SO_2 (equation A.3). A few of these materials are listed below:

Building stone: leaching, deterioration, discoloration;

Fabric, leather, dyes: weakening, embrittlement,
fading;

Metals: surface deterioration, net loss of metal
(esp. zinc);

Paper: fiber deterioration;

Paint: discoloration;

Rubber: cracking, loss of elasticity.

2. Damage to Vegetation

A large number of plants, particularly some leafy commercial species, suffer serious leaf damage (bleaching and chlorosis) under the action of atmospheric SO_2 . The injury threshold varies according to species but for the more susceptible, such as pear trees, the maximum level for continuous eight-hour exposure is about 0.3 ppm.

3. Effects on Animals

As with plants, animals differ markedly in their susceptibility to inspired SO_2 . Primarily, SO_2 acts as an irritant to the respiratory system, damaging mucous linings of the upper tract. Relatively high levels (3.5 ppm) are necessary to produce a health hazard to the healthy adult human, but the aged (and those suffering from chronic respiratory or cardiovascular diseases) are much more susceptible.

D. CONTROL OF SO_2 POLLUTION

Suggested methods for the reduction and control of SO_2 emissions include:

use of low-sulfur fuels;

desulfurization of fuels before burning;
stack gas scrubbing;
use of higher stacks (at present the most effective
and least expensive method available for reducing
ground-level concentrations).

All are partial answers at present, and the high cost and limited availability of such systems urges the development of alternate solutions. The availability of a workable diffusion model could permit the application of a regional "preferred location" scheme; power-generating loads would be shifted from plants in a region of high potential accumulation to those in areas of reduced potential, based upon prevailing meteorological conditions.

BIBLIOGRAPHY

1. Archer, D. A., 1974: Personal communication, 14 Jan.
2. Aziz, K., L. A. Carr, R. D. Rowe and J. Wallis, 1973: "Computer Modelling of Pollution from Atmospheric Sources", Univ. of Calgary Press.
3. Briggs, G. A., 1969: "Plume Rise", U.S. Atomic Energy Commission.
4. Darling, D. D., 1971: "Local Wind Regimes As Related to Medium- and Large-Scale Circulations", Unpublished research.
5. Douglas, J. Jr., 1962: "Alternating Direction Methods for Three Space Variables", Numerische Mathematik, Vol. 4, No. 1.
6. Duffin, J., 1973: "Interim Report on EPA Program AIREC for NARF-NAS-NorIs Complex, San Diego", Unpublished report.
7. Edinger, J., 1963: "Modification of the Marine Layer over Coastal Southern California", Journal of Applied Meteorology, Vol. 2, No. 6.
8. Golder, D., 1972: "Relations Among Stability Parameters in the Surface Layer", Boundary-Layer Meteorology, Vol. 3, No. 1.
9. Haltiner, G. J., 1971: Numerical Weather Prediction, Wiley and Sons.
10. Haltiner, G. J., and F. L. Martin, 1957: Dynamical and Physical Meteorology, McGraw-Hill.
11. Hilst, G. R., 1970: "Sensitivities of Air Quality Prediction to Input Errors and Uncertainties", Proceedings of Symposium on Multiple-Source Urban Diffusion Models, U.S. Environmental Protection Agency, AP-86.
12. Holland, J. Z., 1967: "Radioactive Air Pollution in the 9D's", Proceedings of the U.S. Atomic Energy Commission Meteorological Information Meeting, Canadian AEC Pub. AECL-2787.
13. Holzworth, G. C., 1972: "Mixing Heights, Wind Speeds and Potential for Urban Air Pollution throughout the Contiguous United States", Office of Air Programs Pub. No. AR-101.

14. Kraft, J. C., 1971: "An Investigation into the Effect of an Industrial Heat Source on Local Atmospheric Conditions", Master's thesis, U.S. Naval Postgraduate School.
15. Lamb, R. G., 1971: "Numerical Modelling of Urban Air Pollution", PhD thesis, UCLA.
16. Lamb, R. G., 1973: Personal communication, 30 Nov.
17. Lettau, H. H., 1970: "Physical and Meteorological Basis for Mathematical Models of Urban Diffusion Processes", Proceedings of Symposium on Multiple-Source Urban Diffusion Models, U.S. EPA, AP-86.
18. Luers, J. K., 1973: "A Model of Wind Shear and Turbulence in the Surface Boundary Layer", NASA Contractor Report, NASA CR-2288.
19. Mitchell, A. F., 1969: Computational Methods in Partial Differential Equations, Wiley and Sons.
20. Molencamp, C. R., 1968: "Accuracy of Finite Difference Methods Applied to the Advection Equation", Journal of Applied Meteorology, Vol. 7, No. 4.
21. Monin, A. S. and A. M. Yaglom, 1965: Statistical Fluid Mechanics, Vol. I, MIT Press (1971 English translation).
22. Moses, H. and J. E. Carson, "Stack Design Parameters Influencing Plume Rise", Journal of the Air Pollution Control Assoc.
23. Neiburger, M., D. Johnson and C. W. Chien, 1961: "Studies of the Structure of the Atmosphere over the Eastern Pacific Ocean in Summer", Univ. of Calif. Publications in Meteorology, U. of Calif.
24. Panofsky, H. A. and J. L. Lumley, 1964: The Structure of Atmospheric Turbulence, Wiley and Sons.
25. Pasquill, F., 1961: "The Estimation of the Dispersion of Windborne Information", Meteorology Magazine, London, Vol. 90.
26. Randerson, D., 1970: "A Numerical Experiment in Simulating the Transport of Sulfur Dioxide through the Atmosphere", Atmospheric Environment, Vol. 4, No. 10.
27. Read, R. G., 1972: "Air Flow Land-Sea-Air Interface Monterey Bay Calif - 1971", Contributions from the Moss Landing Marine Laboratories, Pub. 29.

28. Schroeder, M. J., M. A. Fosberg, O. P. Cramer, and C. A. O'Dell, 1967: "Marine Air Invasion of the Pacific Coast: A Problem Analysis", Bull. Amer. Meteorological Society, Vol. 48.
29. Shieh, L. J., 1973: Personal communication, Nov. 22.
30. Shieh, L. J., B. Davidson, and J. P. Friend, 1970: "A Model of Diffusion in Urban Atmospheres: SO₂ in Greater New York", Proceedings of Symposium on Multiple-Source Urban Diffusion Models, U.S. EPA, AP-86.
31. Shir, C. C., 1973: Personal communication, Nov. 22.
32. Shir, C. C. and L. J. Shieh, 1973: "A Generalized Urban Air Pollution Model and Its Application to the Study of SO₂ Distributions in the St. Louis Metropolitan Area", IBM Research Report, RJ-1227.
33. Stern, A. C., 1968: Air Pollution, Vol I.: Air Pollution and Its Effects, 2nd ed., Academic Press.
34. Stoker, H. S. and S. L. Seager, 1972: Environmental Chemistry: Air and Water Pollution, Scott, Foresman and Co.
35. Turner, D. B., 1969: "Workbook of Atmospheric Dispersion Estimates", U.S. Dept of Health, Educ. and Welfare, Pub. Health Service.
36. Turner, D. B., 1964: "A Diffusion Model for Urban Areas", Journ. of Appl. Meteor., Vol. 3, No. 1.
37. Van der Hofen, I., 1967: "Atmospheric Transport and Diffusion at Coastal Sites", Proceedings of U.S. AEC Meteorological Information Meeting, Canadian AEC, Pub AECL-2787.
38. Williamson, S. J., 1973: Fundamentals of Air Pollution, Addison-Wesley Publishers.

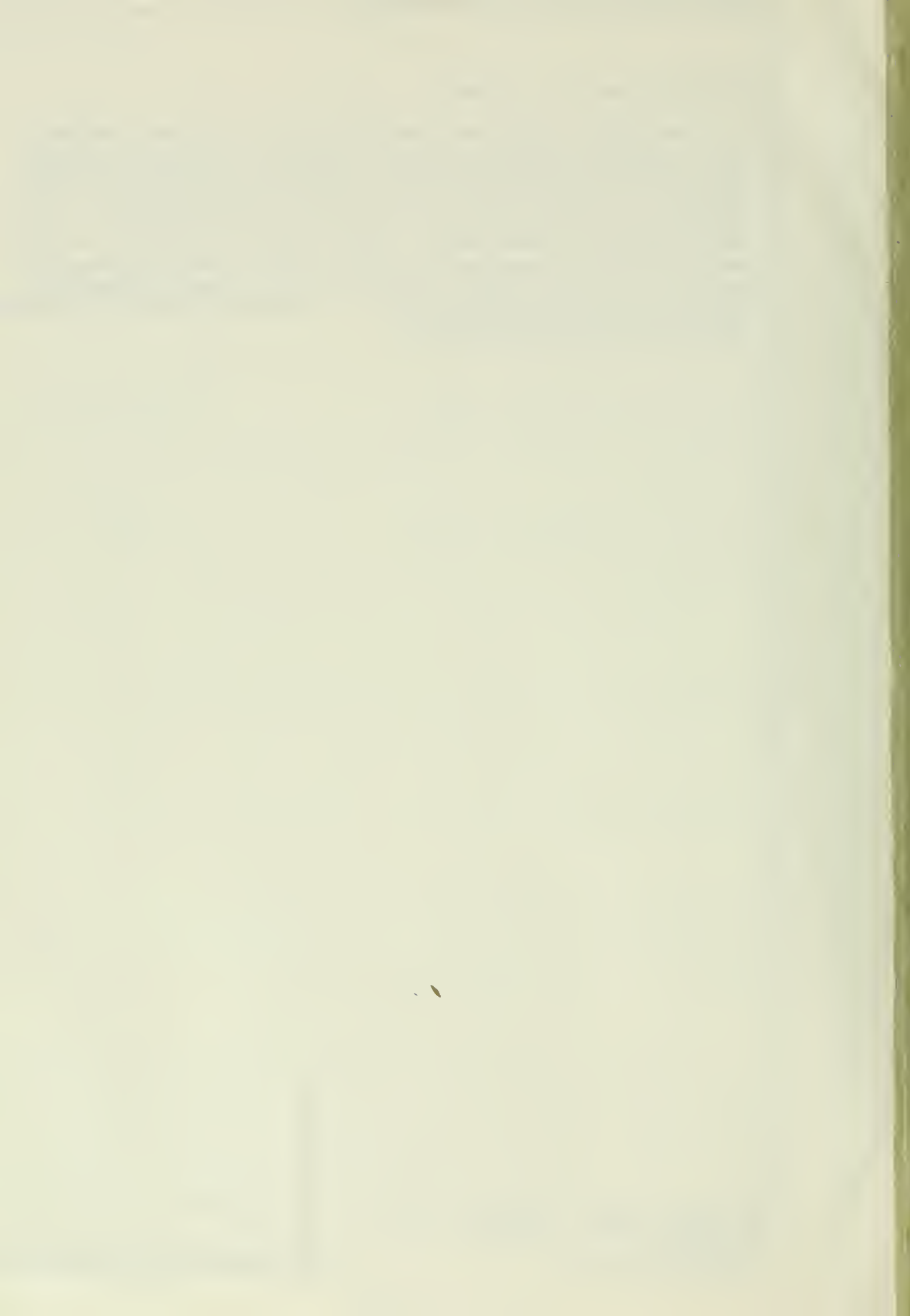
INITIAL DISTRIBUTION LIST

	No. Copies
1. Defense Documentation Center Cameron Station Alexandria, Virginia 22314	2
2. Library, Code 0212 Naval Postgraduate School Monterey, California 93940	2
3. Professor G. J. Haltiner Meteorology Department, Code 51 Naval Postgraduate School Monterey, California 93940	1
4. Professor C. L. Taylor Meteorology Department, Code 51 Naval Postgraduate School Monterey, California 93940	5
5. Professor R. L. Haney Meteorology Department Code 51 Naval Postgraduate School Monterey, California 93940	1
6. Mr. R. C. Puckett Pacific Gas and Electric Co. Moss Landing, California 95039	1
7. LT Michael A. McCallister USS Okinawa (LPH 3) FPO San Francisco, California 96601	2
8. Naval Oceanographic Office Library (Code 3330) Washington, D. C. 20373	1
9. Commander, Naval Weather Service Command Naval Weather Service Headquarters Washington Navy Yard Washington, D. C. 20390	1

REPORT DOCUMENTATION PAGE		READ INSTRUCTIONS BEFORE COMPLETING FORM
1. REPORT NUMBER	2. GOVT ACCESSION NO.	3. RECIPIENT'S CATALOG NUMBER
4. TITLE (and Subtitle) A Theoretical Study of Meteorological Effects on the Dispersion of Atmospheric Contaminants in the Coastal Environment		5. TYPE OF REPORT & PERIOD COVERED Master's Thesis March 1974
		6. PERFORMING ORG. REPORT NUMBER
7. AUTHOR(s) Michael Alan McCallister		8. CONTRACT OR GRANT NUMBER(s)
9. PERFORMING ORGANIZATION NAME AND ADDRESS Naval Postgraduate School Monterey, California 93940		10. PROGRAM ELEMENT, PROJECT, TASK AREA & WORK UNIT NUMBERS
11. CONTROLLING OFFICE NAME AND ADDRESS Naval Postgraduate School Monterey, California 93940		12. REPORT DATE March 1974
		13. NUMBER OF PAGES 64
14. MONITORING AGENCY NAME & ADDRESS (if different from Controlling Office) Naval Postgraduate School Monterey, California 93940		15. SECURITY CLASS. (of this report) Unclassified
		15a. DECLASSIFICATION/DOWNGRADING SCHEDULE
16. DISTRIBUTION STATEMENT (of this Report) Approved for public release; distribution unlimited.		
17. DISTRIBUTION STATEMENT (of the abstract entered in Block 20, if different from Report)		
18. SUPPLEMENTARY NOTES		
19. KEY WORDS (Continue on reverse side if necessary and identify by block number) Air/Atmospheric Pollution, Pollution Meteorology, Plume Dispersal, Gaussian Diffusion, Alternating Direction Implicit Model, Diffusion Modelling.		
20. ABSTRACT (Continue on reverse side if necessary and identify by block number) Present numerical models describing pollutant diffusion employ two main approaches to the problem. Gaussian bivariate distributions based on the statistical properties of atmospheric flow have the advantages of simplicity and computational economy. Numerical simulations of diffusion, based on the continuity equation and conservation relations, allow a more precise description of atmospheric turbulent flow.		

Block 20 Abstract (CONT)

The thesis examines numerical models of each method. The governing equations are discussed, with basic assumptions which permit reasonable simplifications to be made. Results of both models are examined qualitatively to describe patterns of marine-layer pollutant dispersal. Calculations from both models reveal wind velocity to be the most critical atmospheric characteristic controlling dispersion. Rates of spreading are also closely related to other measurable meteorological properties such as thermal stability and mixing depth.



Thesis
M16435
c.1

McCallister

149191

A theoretical study
of meteorological ef-
fects on the dispersion
of atmospheric contami-
nants in the coastal
environment.

Thesis
M16435
c.1

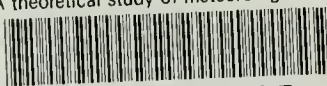
McCallister

149191

A theoretical study
of meteorological ef-
fects on the dispersion
of atmospheric contami-
nants in the coastal
environment.

thesM16435

A theoretical study of meteorological ef



3 2768 001 88699 7

DUDLEY KNOX LIBRARY